DOI: 10.3969/j.issn.1673-3185.2017.06.019 **http**: // english.ship-research.com

Translated from: HE H B, LIU H L. Radial electromagnetic force calculation of induction motor based on multi-loop theory[J]. Chinese Journal of Ship Research, 2017, 12(6): 127-133.

Radial electromagnetic force calculation of induction motor based on multi-loop theory

HE Haibo, *LIU Hailong*

Wuhan Institute of Marine Electric Propulsion, Wuhan 430064, China

Abstract: [**Objectives**] In order to study the vibration and noise of induction motors, a method of radial electromagnetic force calculation is established on the basis of the multi-loop model. [**Methods**] Based on the method of calculating air-gap magneto motive force according to stator and rotor fundamental wave current, the analytic formulas are deduced for calculating the air-gap magneto motive force and radial electromagnetic force generated in accordance with any stator winding and rotor conducting bar current. The multi-loop theory and calculation method for the electromagnetic parameters of a motor are introduced, and a dynamic simulation model of an induction motor built to achieve the current of the stator winding and rotor conducting bars, and obtain the calculation formula of radial electromagnetic force. The radial electromagnetic force and vibration are then estimated. [**Results**] The experimental results indicate that the vibration acceleration frequency and amplitude of the motor are consistent with the experimental results. [**Conclusions**] The results and calculation method can support the low noise design of converters.

Key words: induction motor; multi-loop; magneto motive force; radial electromagnetic force

CLC number: U665.11

0 Introduction

Induction motor is widely used in actuating units due to its simple structure, high reliability and low cost, which also brings noise problems. Vibration noise of induction motor is divided into mechanical noise, electromagnetic noise and aerodynamic noise. Among them, the electromagnetic noise generated by radial electromagnetic force has always been the focus of attention. The radial electromagnetic force of induction motor is produced by the harmonic of stator and rotor fields, and its composition is complicated. As the application of speed adjusting by converter increases in the field of induction motors, the current harmonic introduced by converters makes the electromagnetic vibration noise source of induction motor more complicated.

In order to study the electromagnetic vibration noise generated by the radial electromagnetic force of induction motor, some scholars studied the electromagnetic vibration problem of the conventional induction motor by combining analytical method with modal experiment [1-4]. All of these studies focus on the electromagnetic force under sinusoidal wave power supply, but the vibration under the power supply of converter is not elaborate. With the increase of the current harmonic components of converter, the harmonic components contained in the electromagnetic force also increase, and even the components with the same order and frequency may exist. It is unrealistic to use the analytical method to calculate the amplitude of each harmonic component. With the development of finite element computation technology, some scholars have begun to use finite element method to study the radial electromagnetic force wave problem of induction motor under power frequency and converter supply [5-8]. However, this kind of method cannot directly reveal the relationship between the radial electromagnetic force and the electromagnetic parameters of motor, and cannot distinguish the sources of electromagnetic force harmonics.

In order to analyze the radial electromagnetic

Received: 2017-03-31

Author(s): HE Haibo (Corresponding author), male, born in 1986, master, engineer. Research interest: low-noise motor design. E-mail: hhbhhy@126.com

LIU Hailong, male, born in 1981, master, engineer. Research interest: low-noise motor design

force under power supply with arbitrary voltage waveform more comprehensively, it is necessary to obtain stator winding and rotor bar current. Therefore, multi-loop theory can be used to calculate the stator winding and rotor bar current of induction motor. Reference [9] presented a linear expression of the mutual inductance parameters, which was simple in form and easy to be implemented, and can exhaust all the harmonic components without truncation error. However, the analytical formula is only applicable for the case of full pitch, $q=1$ (q is the number of slots per pole and per phase). The rules of the magnetomotive force waveforms in this case are simple to calculate, so the analytical formula can be obtained directly. The situation is much more complicated when there is a non-full pitch or $q\neq 1$ in the motor, so it is necessary to derive a general formula.

This paper aims to deduce the general formula for multi-loop simulation model of induction motor, and uses Matlab to simulate the motor and obtain real-time current in stator and rotor windings, so as to calculate the real-time distribution of air-gap field and use the Maxwell stress method to obtain the order and magnitude of each harmonic of radial electromagnetic force.

1 Multi-loop model

First, the multi-loop theory is used to calculate the actual current waveforms of stator windings and rotor bars. If the stator winding of each phase in induction motor is regarded as a loop, and every two bars and the end ring of the rotor are regarded as a component to form a large circuit, a multi-loop analysis simulation model can be established. For the convenience of calculation, it is assumed that the effects of ferromagnetic material saturation, hysteresis and eddy current, and the skin effect of conductive material are negligible.

1.1 Stator voltage equation

According to the circuit theory, for M-phase induction motor, the stator voltage equation can be listed as:

$$\boldsymbol{U}_{\mathrm{s}}=\boldsymbol{R}_{\mathrm{s}}\boldsymbol{I}_{\mathrm{s}}+\frac{\mathrm{d}\boldsymbol{\psi}_{\mathrm{s}}}{\mathrm{d}t} \tag{1}$$

where $\boldsymbol{U}_{\mathrm{s}}=[u_{\mathrm{s}1}\ u_{\mathrm{s}2}\ \cdots\ u_{\mathrm{s}M}]^{\mathrm{T}}$ is the stator voltage; $\boldsymbol{R}_{\mathrm{s}}=r_{\mathrm{s}}\boldsymbol{E}_{M\times M}$ is the impedance matrix of stator, in which r_{s} is phase resistance of stator, $\boldsymbol{E}_{M\times M}$ is the cell matrix of $M\times M$ dimensions; $\boldsymbol{I}_{\mathrm{s}}=[i_{\mathrm{s}1}\ i_{\mathrm{s}2}\ \cdots\ i_{\mathrm{s}M}]^{\mathrm{T}}$ is stator current; $\boldsymbol{\psi}_{\mathrm{s}}=[\psi_{\mathrm{s}1}\ \psi_{\mathrm{s}2}\ \cdots\ \psi_{\mathrm{s}M}]^{\mathrm{T}}$ is the stator flux linkage.

1.2 Rotor voltage equation

For a cage rotor with N bars, it can be regarded as N loops. The resistance of each bar is r_{b}, and the resistance of the end ring between two bars is r_{e}, as shown in Fig. 1. According to the circuit diagram, the following equation can be obtained:

$$\boldsymbol{R}_{\mathrm{r}}\boldsymbol{I}_{\mathrm{r}}+\frac{\mathrm{d}\boldsymbol{\psi}_{\mathrm{r}}}{\mathrm{d}t}=0 \tag{2}$$

where $\boldsymbol{I}_{\mathrm{r}}=[i_{\mathrm{r}1}\ i_{\mathrm{r}2}\ \cdots\ i_{\mathrm{r}N}]^{\mathrm{T}}$ is the current of each bar of the rotor; $\boldsymbol{\psi}_{\mathrm{r}}=[\psi_{\mathrm{r}1}\ \psi_{\mathrm{r}2}\ \cdots\ \psi_{\mathrm{r}N}]^{\mathrm{T}}$ is the rotor flux linkage; $\boldsymbol{R}_{\mathrm{r}}$ is the resistance matrix of rotor,

$$R_{\mathrm{r}}=\begin{bmatrix} r_{\mathrm{r}} & -r_{\mathrm{b}} & 0 & \cdots & -r_{\mathrm{b}} \\ -r_{\mathrm{b}} & r_{\mathrm{r}} & -r_{\mathrm{b}} & \cdots & 0 \\ 0 & -r_{\mathrm{b}} & r_{\mathrm{r}} & \cdots & 0 \\ \vdots & \vdots & \vdots & & \vdots \\ -r_{\mathrm{b}} & 0 & 0 & \cdots & r_{\mathrm{r}} \end{bmatrix} \tag{3}$$

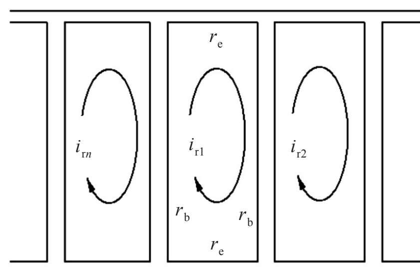

Fig.1 Rotor circuit

1.3 Flux linkage equation

The stator/rotor flux linkage equation is:

$$\begin{bmatrix}\boldsymbol{\psi}_{\mathrm{s}}\\ \boldsymbol{\psi}_{\mathrm{r}}\end{bmatrix}=\begin{bmatrix}\boldsymbol{L}_{\mathrm{ss}} & \boldsymbol{L}_{\mathrm{sr}}\\ \boldsymbol{L}_{\mathrm{sr}}^{\mathrm{T}} & \boldsymbol{L}_{\mathrm{rr}}\end{bmatrix}\begin{bmatrix}\boldsymbol{I}_{\mathrm{s}}\\ \boldsymbol{I}_{\mathrm{r}}\end{bmatrix} \tag{4}$$

where $\boldsymbol{L}_{\mathrm{ss}}$ is the mutual inductance matrix of stator winding; $\boldsymbol{L}_{\mathrm{sr}}$ is the mutual inductance matrix between stator and rotor loops; $\boldsymbol{L}_{\mathrm{rr}}$ is the mutual inductance matrix between rotor bars. The equation of state can be rewritten as:

$$\begin{bmatrix}\boldsymbol{U}_{\mathrm{s}}\\ \boldsymbol{U}_{\mathrm{r}}\end{bmatrix}=\begin{bmatrix}\boldsymbol{R}_{\mathrm{s}} & 0\\ 0 & \boldsymbol{R}_{\mathrm{r}}\end{bmatrix}\begin{bmatrix}\boldsymbol{I}_{\mathrm{s}}\\ \boldsymbol{I}_{\mathrm{r}}\end{bmatrix}+\frac{\mathrm{d}}{\mathrm{d}t}\left(\begin{bmatrix}\boldsymbol{L}_{\mathrm{ss}} & \boldsymbol{L}_{\mathrm{sr}}\\ \boldsymbol{L}_{\mathrm{sr}}^{\mathrm{T}} & \boldsymbol{L}_{\mathrm{rr}}\end{bmatrix}\begin{bmatrix}\boldsymbol{I}_{\mathrm{s}}\\ \boldsymbol{I}_{\mathrm{r}}\end{bmatrix}\right)=$$
$$\left(\begin{bmatrix}\boldsymbol{R}_{\mathrm{s}} & 0\\ 0 & \boldsymbol{R}_{\mathrm{r}}\end{bmatrix}+\omega_{\mathrm{r}}\begin{bmatrix}0 & \dfrac{\mathrm{d}\boldsymbol{L}_{\mathrm{sr}}}{\mathrm{d}\theta}\\ \dfrac{\mathrm{d}\boldsymbol{L}_{\mathrm{sr}}^{\mathrm{T}}}{\mathrm{d}\theta} & 0\end{bmatrix}\right)\begin{bmatrix}\boldsymbol{I}_{\mathrm{s}}\\ \boldsymbol{I}_{\mathrm{r}}\end{bmatrix}+\begin{bmatrix}\boldsymbol{L}_{\mathrm{ss}} & \boldsymbol{L}_{\mathrm{sr}}\\ \boldsymbol{L}_{\mathrm{sr}}^{\mathrm{T}} & \boldsymbol{L}_{\mathrm{rr}}\end{bmatrix}\frac{\mathrm{d}}{\mathrm{d}t}\begin{bmatrix}\boldsymbol{I}_{\mathrm{s}}\\ \boldsymbol{I}_{\mathrm{r}}\end{bmatrix} \tag{5}$$

where θ is electrical angle of rotor rotation; ω_{r} is the electrical angular velocity of rotor rotation.

1.4 Torque equation

According to the motor theory, the electromagnetic torque $\boldsymbol{T}_{\mathrm{e}}$ of motor is:

$$\boldsymbol{T}_{\mathrm{e}}=p\boldsymbol{I}_{\mathrm{s}}^{\mathrm{T}}\frac{\mathrm{d}\boldsymbol{L}_{\mathrm{sr}}}{\mathrm{d}\theta}\boldsymbol{I}_{\mathrm{r}} \tag{6}$$

where p is the pole number of the motor.

Ignoring the frictional damping torque, the equation of rotor motion is:

$$\frac{\boldsymbol{J}}{p}\frac{\mathrm{d}\omega_{\mathrm{r}}}{\mathrm{d}t}=\boldsymbol{T}_{\mathrm{e}}-\boldsymbol{T}_{\mathrm{L}} \tag{7}$$

where $\boldsymbol{J}$ is the rotational inertia of motor and $\boldsymbol{T}_{\mathrm{L}}$ is the load torque.

2 Inductance calculation

The M-phase induction motor analysis model based on multi-loop theory is given in Section 1, in which the resistance matrix can be given by measured or calculated value and is assumed to have no change during the operation of the motor. Each mutual inductance parameter and its derivative with respect to the electrical angle need to be calculated.

2.1 Self-inductance and mutual inductance matrix of stator winding

Assuming that the distribution of the magnetomotive force generated by one coil in the stator winding is shown in Fig. 2 and the difference in electrical angles between any two coils Q_1 and Q_2 is $\Delta\theta_{\mathrm{s}}$, the mutual inductance is:

$$L_{Q_1Q_2}=\frac{\psi}{I_{\mathrm{s}}}=\frac{1}{I_{\mathrm{s}}}\int_{\Delta\theta_{\mathrm{s}}}^{\Delta\theta_{\mathrm{s}}+\frac{y}{\tau}}F(\theta_{\mathrm{s}})\frac{\mu_0}{g_{\mathrm{ef}}}D_2 l_{\mathrm{ef}}\mathrm{d}\theta_{\mathrm{s}} \tag{8}$$

where ψ is the flux linkage of 2 coils; y is the coil pitch; τ is the pole pitch; $F(\theta_{\mathrm{s}})$ is the magnetomotive force generated by coil Q_1; μ_0 is the permeability of vacuum; g_{ef} is the effective length of air gap; D_2 is the inner diameter of stator; l_{ef} is the effective length of core.

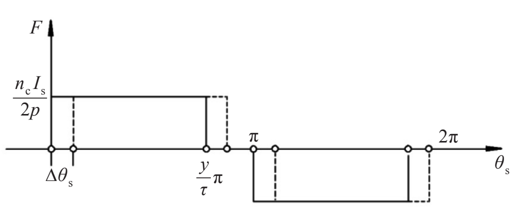

Fig.2 Magnetomotive force of a slot coil

For real motors, the value of $F(\theta_{\mathrm{s}})$ is constant and $\Delta\theta_{\mathrm{s}}$ is related to each coil position and does not change with time, so the integral result is a finite number of discrete values. These discrete values can be programmed to form a table and calculated by table lookup method. Mutual inductance between any two phase coils s_{m1} and s_{m2} is:

$$L_{s_{m1},s_{m2}}=\sum_{Q_1=1}^{q1}\sum_{Q_2=1}^{q1}L_{s_{m1}Q_1,s_{m2}Q_2} \tag{9}$$

Taking into account the leakage inductance of stator winding, when $s_{m1}=s_{m2}$, the leakage inductance value needs to be added.

2.2 Mutual inductance matrix between the rotor bar loop

The distribution of the air-gap magnetomotive force generated by a bar loop of the rotor is shown in Fig. 3, where the circle represents the bar cross-section. Supposing the electrical angle between two bars is $\Delta\theta_{\mathrm{r}}$, Fig. 3 shows the relationship between the mutual inductance of two bar loops and the electrical angle $\Delta\theta_{\mathrm{r}}$. Since $\Delta\theta_{\mathrm{r}}$ is discrete, the mutual inductance between any two corresponding bars is also discrete.

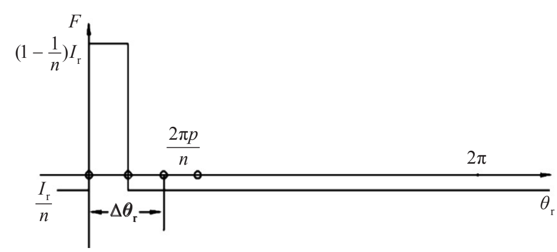

Fig.3 Magnetomotive force of rotor

Considering the leakage inductance between the rotor bar loops, the mutual inductance between the r_{n1} th bar loop and the r_{n2} th bar loop can be obtained as:

$$L_{r_{n1},r_{n2}}=\frac{\psi}{I_{\mathrm{r}}}=\frac{1}{I_{\mathrm{r}}}\int_{\Delta\theta_{\mathrm{r}}}^{\Delta\theta_{\mathrm{r}}+\frac{2\pi p}{N}}F(\theta_{\mathrm{r}})\frac{\mu_0}{g_{\mathrm{ef}}}D_2 l_{\mathrm{ef}}\mathrm{d}\theta_{\mathrm{r}} \tag{10}$$

where $F(\theta_{\mathrm{r}})$ is the magnetomotive force generated by a bar loop.

Eq. (10) is relatively simple. After integration, it can be obtained as:

$$L_{r_{n1},r_{n2}}=\begin{cases}L_{\mathrm{r\,max}}+2(L_{\mathrm{e}}+L_{\mathrm{b}}), & r_{n1}=r_{n2}\\ -L_{\mathrm{r\,min}}-L_{\mathrm{b}}, & |r_{n1}-r_{n2}|=1\text{, or } |r_{n1}-r_{n2}|=N-1\\ -L_{\mathrm{r\,min}}, & \text{others}\end{cases} \tag{11}$$

where L_{e} is the leakage inductance generated by the end; L_{b} is the leakage inductance generated by a bar, and

$$L_{\mathrm{r\,max}}=\left(1-\frac{1}{N}\right)\frac{\mu_0}{g_{\mathrm{ef}}}\frac{\pi D_2}{N}l_{\mathrm{ef}}\text{ ,}$$

$$L_{\mathrm{r\,min}}=\frac{1}{N^2}\frac{\mu_0}{g_{\mathrm{ef}}}\pi D_2 l_{\mathrm{ef}} \tag{12}$$

2.3 Mutual inductance between the stator and the rotor

It is assumed that the magnetomotive force distribution of an air gap generated by a phase of stator winding is shown in Fig. 4, where the black circle represents the bar section of a loop of the rotor, and the electrical angle difference between it and the stator winding is $\Delta\theta_{sr}$:

$$\Delta\theta_{sr}=\Delta\theta_{sr}(0)+\int_0^t\omega_r(\tau)\mathrm{d}\tau \tag{13}$$

where $\Delta\theta_{sr}(0)$ is the initial electrical angle difference. When $\Delta\theta_{sr}$ changes within a period, the mutual inductance between the stator and the rotor is:

$$L_{sr}=\frac{\psi}{I_s}=\frac{1}{I_s}\int_{\Delta\theta_{sr}-\frac{\pi p}{N}}^{\Delta\theta_{sr}+\frac{\pi p}{N}}F(\theta_s)\frac{\mu_0}{g_{ef}}D_2 l_{ef}\mathrm{d}\theta_s \tag{14}$$

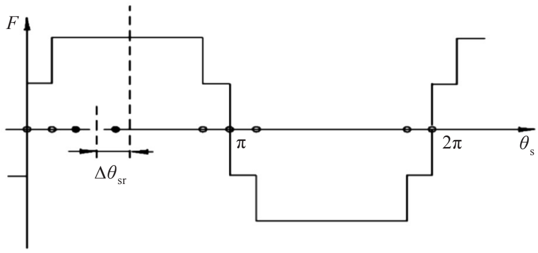

Fig.4 Stator rotor mutual inductance

The calculation formula of $L_{sr\max}$ is:

$$L_{sr\max}=\frac{n_s}{2p}\frac{\mu_0}{g_{ef}}\frac{\pi D_2}{N}l_{ef} \tag{15}$$

where n_s is the number of series branches of stator winding in each phase.

2.4 Derivative of stator/rotor mutual inductance with respect to electrical angle

According to the mutual inductance between the stator and the rotor, the derivative of the mutual inductance parameter with respect to the electrical angle can be given as:

$$\frac{\mathrm{d}L_{sr}}{\mathrm{d}\theta}=\frac{\Delta L_{sr}}{\Delta\theta} \tag{16}$$

After calculating each mutual inductance parameter and its derivative with respect to the electrical angle, the simulation model of the converter motor can be constructed, and the waveform of all the loop current of motor stator and rotor with time can be obtained, as well as the distribution of the electromagnetic force of the motor along the air-gap circumference.

3 Calculation of radial magnetomotive force

Multi-phase motors are usually supplied by converters. Due to the use of switching devices in the converters, the output voltage contains a large amount of harmonics. The traditional analytical method can only solve the electromagnetic force under the fundamental power supply, while the electromagnetic force generated by the harmonic current is neglected. To calculate the electromagnetic force generated by the harmonic current, the current waveform of the motor is obtained through simulation calculation. According to the spatial location of current waveform, the flux density waveform of the motor can be obtained, as well as the electromagnetic force of motor in the converter. When this method is used, the amplitude of each harmonic is not calculated any more. Instead, the magnetomotive force generated by each phase coil is directly added to obtain the air-gap magnetomotive force.

When power is supplied by the converter, the fundamental magnetomotive force generated by the s_m th phase winding is expressed as:

$$f_{s_m}(\alpha,t)=\frac{2}{\pi p}N_a k_{w1} i_{s_m}(t)\cos\{p[\alpha-\phi(s_m)]\} \tag{17}$$

where N_a is the number of series branches of each phase winding; k_{w1} is the fundamental winding coefficient of the stator winding; $i_{s_m}(t)$ is the real-time magnitude of the current of the s_m th phase winding; α is the space angle of air-gap circumference, and $\phi(s_m)$ is the spatial position of the center line of the s_m th phase winding. Similar to the sinusoidal wave power supply, the magnetomotive force waveform of v th-order harmonic is:

$$f_{s_m v}(\alpha,t)=\frac{2}{\pi v p}Nk_{wv} i_{s_m}(t)\cos\{pv[\alpha-\phi(s_m)]\} \tag{18}$$

where k_{wv} is the v th-order harmonic winding coefficient of stator winding. So, the synthesized magnetomotive force of stator winding is:

$$f_s(\alpha,t)=\sum_{s_m=1}^{M}\sum_{v=2Mk\pm1}^{\infty}f_{s_m v}(\alpha,t) \tag{19}$$

where, $k=1,2,3\cdots\cdots$

The magnetomotive force of rotor is also expressed in a similar way and the fundamental magnetomotive force generated by the current of r_n th bar is expressed as:

$$f_{r_n}(\alpha,t)=\frac{2}{\pi p}N_2 k_{w2} i_{r_n}(t)\cos\{p[\alpha-2\pi r_n/N+\phi_{r_n}(t)]\} \tag{20}$$

where $N_2=1$, k_{w2} is the winding coefficient of bar loop; $i_{r_n}(t)$ is the real-time current of the r_n th rotor loop; $\phi_{r_n}(t)$ is the spatial position of the r_n th rotor loop. Similar to the sinusoidal wave power supply, the magnetomotive force waveform of the uth-order harmonic is:

$$f_{r_n u}(\alpha,t)=\frac{2}{\pi p u}N_2 k_{wru} i_{r_n}(t)\cos\{pu[\alpha-2\pi r_n/N+\phi_{r_n}(t)]\} \tag{21}$$

So, the synthesized magnetomotive force of rotor winding is:

$$f_r(\alpha, t) = \sum_{r_n=1}^{N} \sum_{u=kN/p\pm1}^{\infty} f_{r_n u}(\alpha, t) \qquad (22)$$

The synthesized air-gap magnetomotive force is:

$$f(\alpha, t) = f_s(\alpha, t) + f_r(\alpha, t) \qquad (23)$$

3.2 Air-gap permeance calculation

The relative permeance of the physical air gap of induction motor increases with the Carter's coefficient. Because of the skin effect caused by slotting, the air-gap field corresponding to the teeth is larger than that without slots. According to Reference [10], only considering the stator slotting, the air-gap permeance is:

$$\Lambda(\alpha) = \Lambda_0 + \sum_{k=1}^{\infty} \Lambda_{1k} k Z_1 \alpha \qquad (24)$$

where Λ_0 is the constant part of air-gap permeance; Λ_{1k} is the amplitude of the k^{th}-order tooth harmonic permeance of the stator when the rotor is smooth; Z_1 is the slot number of stator.

Similarly, if the inner surface of the stator is smooth, the rotor has a slot, and the rotor rotates at a rotation speed Ω_2 relative to the stator, the main component of the air-gap permeance can be expressed as:

$$\Lambda(\alpha, t) = \Lambda_0 + \sum_{k=1}^{\infty} \Lambda_{2k} kN(\alpha - \Omega_2 t) \qquad (25)$$

where Ω_2 is mechanical angular velocity of rotor; Λ_{2k} is the amplitude of the k^{th}-order tooth harmonic permeance when the stator is smooth.

The synthesized air-gap permeance is:

$$\Lambda(\alpha, t) = \Lambda_0 \left(1 + \sum_{k=1}^{\infty} \frac{\Lambda_{1k}}{\Lambda_0} k Z_1 \alpha\right) \left[1 + \sum_{k=1}^{\infty} \frac{\Lambda_{2k}}{\Lambda_0} kN(\alpha - \Omega_2 t)\right] \qquad (26)$$

The relationship between air-gap magnetic flux density $b(\alpha, t)$ and magnetomotive force $f(\alpha, t)$ is:

$$b(\alpha, t) = f(\alpha, t) \Lambda(\alpha, t) \qquad (27)$$

Based on Maxwell stress tensor method, the radial electromagnetic force per unit area at any point in the air gap is:

$$p_r(\alpha, t) \approx \frac{b^2(\alpha, t)}{2\mu_0} \qquad (28)$$

3.3 Two-dimensional Fourier analysis of electromagnetic force

After obtaining the distribution of the electromagnetic force of the motor through analysis, a two-dimensional array containing time and space components is obtained. The traditional Fourier analysis can only take the spatial distribution of electromagnetic force at a certain moment for spatial analysis, or take the time distribution of electromagnetic force at a certain spatial location for frequency analysis. However, the same-order electromagnetic force may contain harmonics of different frequencies and electromagnetic forces of the same frequency may contain different orders of components as well. The influence of these harmonics and components on the motor vibration is not the same. Therefore, it is necessary to perform Fourier analysis on both the temporal and spatial distribution of electromagnetic force at the same time.

Matlab software can be used to achieve fast two-dimensional Fourier decomposition of discrete data and obtain the spectrum of different orders of electric excitation force, i.e.,

$$p_r(\alpha, t) = \sum_{k=1}^{\infty} p_{rk}(t) e^{jk\alpha p} = \sum_{k=1}^{\infty} \sum_{f} p_{rkf} e^{jk\alpha p} e^{j2\pi f t} \qquad (29)$$

where $p_{rk}(t)$ is the amplitude of k^{th}-order electromagnetic force varying with time; p_{rkf} is the amplitude of electromagnetic force with the order of k and the frequency of f.

4 Calculation of examples

The working condition of a 3-phase 200 kW motor in a converter is simulated to obtain the radial electromagnetic force, which is then compared with vibration test results. The main parameters of the motor are shown in Table 1.

Table 1 Main parameters of motor

Rated power/kW	200	Number of phase	3
Rated voltage/V	690	Rated speed/($r \cdot min^{-1}$)	500
Phase voltage/V	398	Pole pairs	3
Rated frequency/Hz	25.6	Slot number of stator	72
Rated current/A	200	Slot number of rotor	58

4.1 Simulation results of three-phase motor under sinusoidal power supply

By simulation, the current waveform of the stator and rotor is obtained and shown in Fig. 5. According to Fig. 5, the values of stator current amplitude and rotor speed are consistent with the theoretical values, which proves that the multi-loop model is suitable for the motor and is of high precision.

The magnetomotive force waveform synthesized in electromagnetic force calculation is shown in Fig. 6. As can be seen from Fig. 6, the magnetomotive force waveform of the stator and rotor is a typical step wave, while the harmonic content of synthesized magnetomotive force waveform of air gap is more abundant.

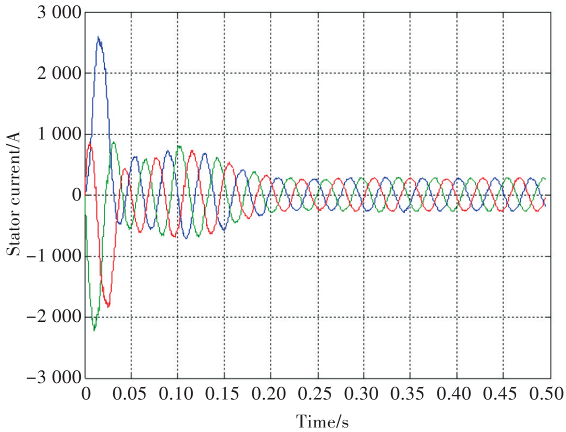

Fig.5 Stator current waveform

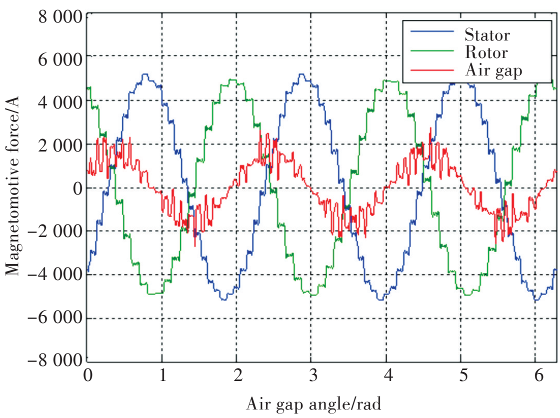

Fig.6 Magnetomotive force waveform of the air gap

Considering the air-gap permeance of stator and rotor, the resulting air-gap field waveform is shown in Fig. 7. It can be seen from Fig. 7 that the harmonic content in the flux density waveform of air gap greatly increases.

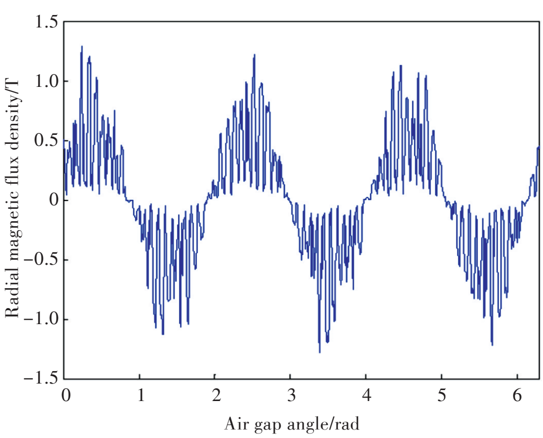

Fig.7 The waveform of air gap flux density

Electromagnetic force is calculated according to the calculation formula of radial electromagnetic force and then the two-dimensional Fourier decomposition is performed. The result is finally shown in Fig. 8. The order and frequency of main harmonics of radial electromagnetic force can be obtained from Fig. 8. Among them, the amplitude of radial electromagnetic force harmonics of 0th order 0 Hz and −6th order 51.2 Hz is the highest. 0th order 0 Hz harmonic component is constant force and does not cause vibration. According to the motor vibration theory, the vibration amplitude of the stator core is inversely proportional to the biquadrate of the electromagnetic force order. The lower the electromagnetic force order is, the higher the amplitude of the generated vibration is. Although −6th order 51.2 Hz harmonic component has high amplitude and high order, but the amplitude of induced electromagnetic vibration is not high. As can be seen from Fig. 8, there are low-order electromagnetic forces such as −2nd order and 2nd order in this motor, which needs close attention.

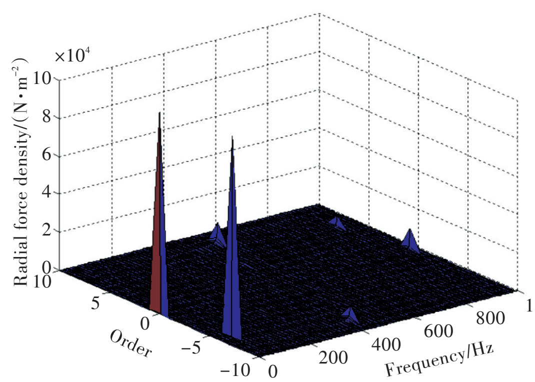

Fig.8 Order and frequency of radial electromagnetic force

The −2nd order and 2nd order electromagnetic force spectra are extracted and shown in Fig. 9. As can be seen from Fig. 9, the motor has 2nd order and −2nd order electromagnetic forces with frequencies of 433 and 535 Hz respectively, which may produce high-amplitude vibration.

4.2 Experiment verification

To verify the results of the theoretical analysis, the experimental platform shown in Fig. 10 is set up. In the platform, the magnetic powder brake with no ob-

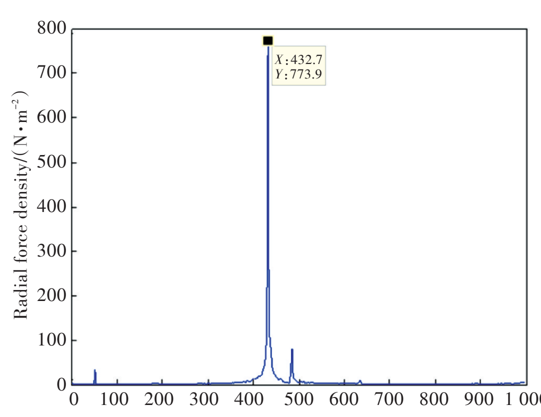

(a) 2nd order

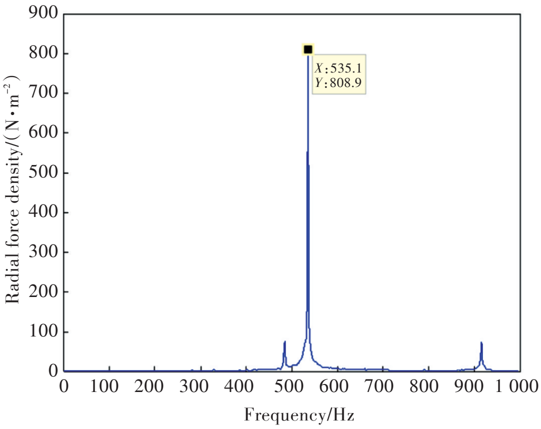

(b) -2^{nd} order

Fig.9 $2^{nd}/-2^{nd}$ order radial electromagnetic force

vious excitation frequency is used as the load of the induction motor. The excitation current of the magnetic particle brake is adjusted to adjust the load size.

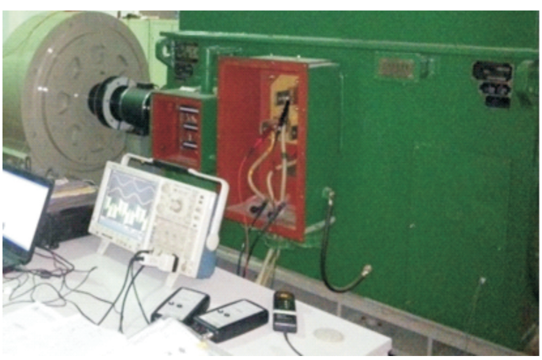

Fig.10 Test site

The vibration acceleration spectrum of motor measured in the experiment is shown in Fig. 11.

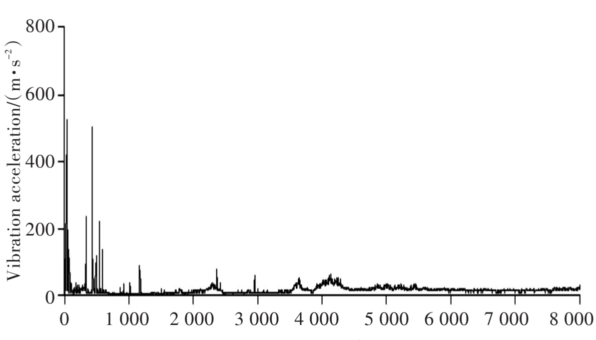

Fig.11 The vibration acceleration spectrum of motor bottom with full load

The calculated results and experimental results of electromagnetic force are shown in Table 2. It can be seen from Table 2 that the results of electromagnetic force frequency agree well with each other. However, the calculated amplitude of vibration acceleration has some errors with the experimental results, which may be caused by the imprecise calculation of structural response.

Table 2 Comparison of calculated and experimental results of electromagnetic force

	32 kW		200 kW	
	Experimental result	calculated result	Experimental result	calculated result
Frenqucy/Hz	444	443	432	432
Amplitude/dB	97.7	87	114	114
Frenqucy/Hz	546	545	534	535
Amplitude/dB	103.5	103	107	114

The traditional method usually establishes the following table (Table 3, the left side of "/" refers to the order and the right side refers to the frequency) to calculate the order and frequency of electromagnetic force. The magnetomotive force of stator contains -51^{st} order, -33^{th} order, -15^{th} order and other harmonics, while the magnetomotive force of rotor contains -55^{th} order, 3^{rd} order, 61^{st} order and other harmonics. The harmonics of stator and rotor affect each other in pairs to generate electromagnetic force. For example, the -51^{st} order harmonic of stator magnetomotive force interacts with the -55^{th} order harmonic of rotor magnetomotive force to produce 4^{th} order 483 Hz radial electromagnetic force. The 57^{th} order harmonic of stator magnetomotive force and the -55^{th} order harmonic of rotor magnetomotive force produce 2^{nd} order 432 Hz radial electromagnetic force.

Table 3 The calculated electromagnetic force order and frequency with traditional methods

Stator magnetic force harmonic	Rotor magnetic force harmonic		
	−55	3	61
−51	4/483	−48/51.2	10/534
−33	22/483	−30/51.2	28/534
−15	40/483	−12/51.2	46/534
3	−52/432	0/0	−58/534
21	−34/432	18/0	−40/534
39	−16/432	36/0	−22/534
57	2/432	54/0	−4/534

In Table 3, there is a 2^{nd} order 432 Hz electromagnetic force, but no 2^{nd} order 534 Hz electromagnetic force. The reason is that when the traditional method is used to calculate the electromagnetic force harmonics, only the influence of the magnetomotive force harmonics of stator is considered, and the interaction between these harmonics and the air-gap permeance harmonics is ignored. For this motor, the 1^{st} order permeance tooth harmonics of stator and the 1^{st} order permeance tooth harmonics of rotor can generate 14^{th} order 483 Hz harmonics and then produce 2^{nd} order 534 Hz electromagnetic force with the -12^{th} order 512 Hz harmonics in Table 3, which is consistent with the experimental results. Therefore, the harmonics calculated by this method are more comprehensive.

5 Conclusions

The calculation method of radial electromagnetic force of induction motor proposed in this paper can obtain the frequency and amplitude of electromagnetic force accurately. Compared with the traditional calculation method, the harmonic amplitude of different orders and frequencies can be calculated through the actual harmonic current amplitude of stator and rotor as many as possible. The calculated results agree well with the experimental results and can be used to calculate the harmonic electromagnetic force of multi-phase motor under converter and the frequency and amplitude of the generated electromagnetic vibration.

References

[1] SHU B F. 电动机的噪声和振动[M]. Translated by SHEN G Q. Beijing: China Machine Press, 1980(in Chinese).

[2] TIMÁR P L. Noise and vibration of electrical machines [M]. Amsterdam: North Holland, 1989.

[3] CHEN Y X, ZHU Z Q, YING S C. 电机噪声的分析和控制 [M]. Hangzhou: Zhejiang University Press, 1987 (in Chinese).

[4] ZHU C S, CHEN Y X. 变频器供电的三相异步电机的噪声特性 [J]. S&M Electric Machines, 1997, 24 (5): 9-12 (in Chinese).

[5] WANG X, QIU A R. Finite element calculation of radial electromagnetic force wave in squirrel-cage asynchronous motors[J]. Transactions of China Electrotechnical Society, 2012, 27(7): 109-117 (in Chinese).

[6] DING H Y, RUAN J J, LIU H H, et al. Simulation research on radial electromagnetic force of inverter-fed induction motor [J]. Micromotors, 2015, 48 (8): 9-12, 31 (in Chinese).

[7] TANG R Y, SONG Z H, YU S B, et al. Study on source of vibration and acoustic noise of permanent magnet machines by inverter [J]. Electric Machines and Control, 2010, 14(3): 12-17 (in Chinese).

[8] WANG D, ZHU C S, FU J J. Analysis of the electromagnetically excited vibration in an asynchronous machine by finite element method [J]. Journal of Vibration and Shock, 2012, 31 (2): 140-144 (in Chinese).

[9] ZHANG J W, ZHU H Q, HUANG Z H, et al. Modeling and simulation of a multiphase concentrated induction machine [J]. Electric Machines and Control, 2010, 14(9): 75-80 (in Chinese).

[10] CHEN S K. 电机设计[M]. Beijing: China Machine Press, 2004(in Chinese).

基于多回路理论的异步电机径向电磁力计算

何海波，刘海龙

武汉船用电力推进装置研究所，湖北 武汉 430064

摘　要：[**目的**] 为了研究变频器供电下的异步电机振动噪声，提出基于多回路模型的异步电机径向电磁力计算方法。[**方法**] 在由定转子基波电流计算气隙磁动势的传统计算方法的基础上，推导由任意定子绕组及转子导条电流计算气隙磁动势及其产生的径向电磁力的解析计算公式。介绍多回路理论及电机各电磁参量的计算方法，建立异步电机多回路动态仿真模型，获得异步电机定子绕组及转子导条电流，推导其产生的径向电磁力的解析公式，并由此计算异步电机径向电磁力，估算其产生的振动。[**结果**] 通过实验验证，发现计算得到的电机振动加速度频率及幅值与实验结果吻合。[**结论**] 所得结论和计算方法可为变频器供电异步电机的低噪声设计提供支持。

关键词：异步电机；多回路；磁动势；径向电磁力